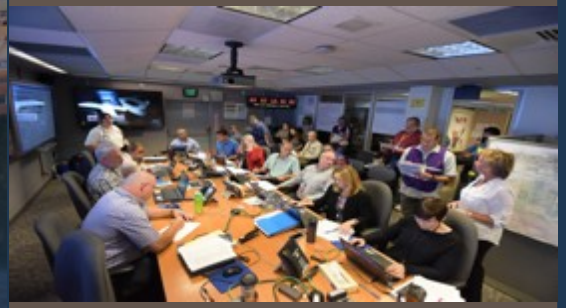

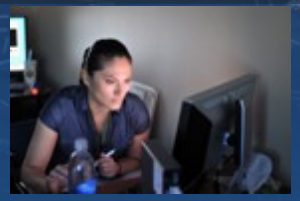

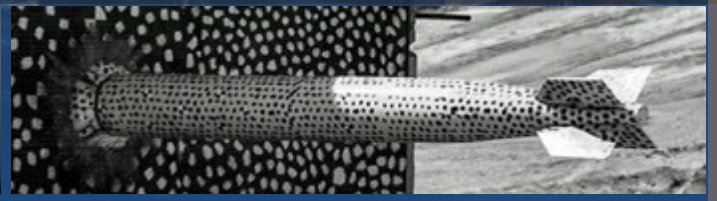

Large-scale theroretical predictions of pressure and temperature ramps in iron

PRESENTED BY

J. Tranchida

Collaborators: S. Nikolov, M.A. Wood, A. Cangi, M.P. Desjarlais, A.P. Thompson

Contact: jtranch@sandia.gov

Sandia National Laboratories is a multimission laboratory managed and operated by National Technology and Engineering Solutions of Sandia LLC, a wholly owned subsidiary of Honeywell International Inc. for the U.S. Department of Energy's National Nuclear Security Administration under contract DE-NA0003525.

Motivations for “magnetic” calculations:

Heat-capacity, alpha iron:

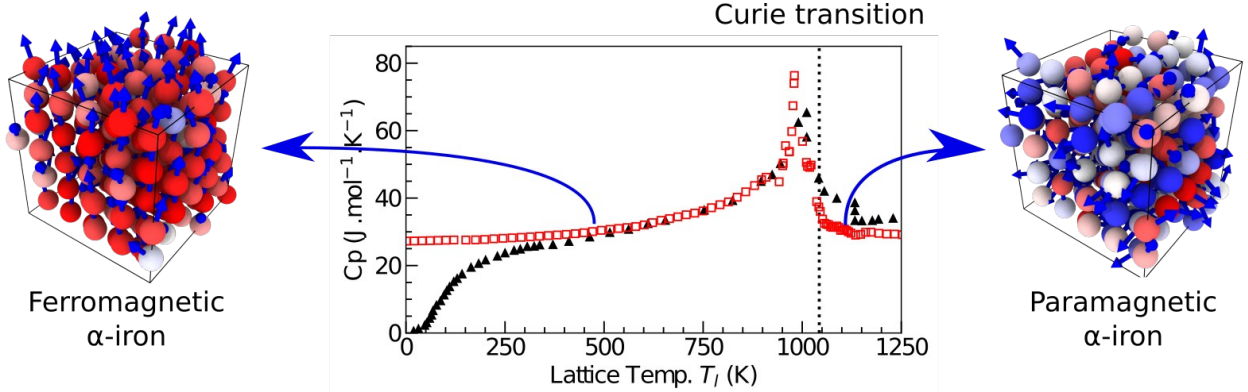

▲ Exp. measurements ☐ Our model

Shear-modulus, alpha iron:

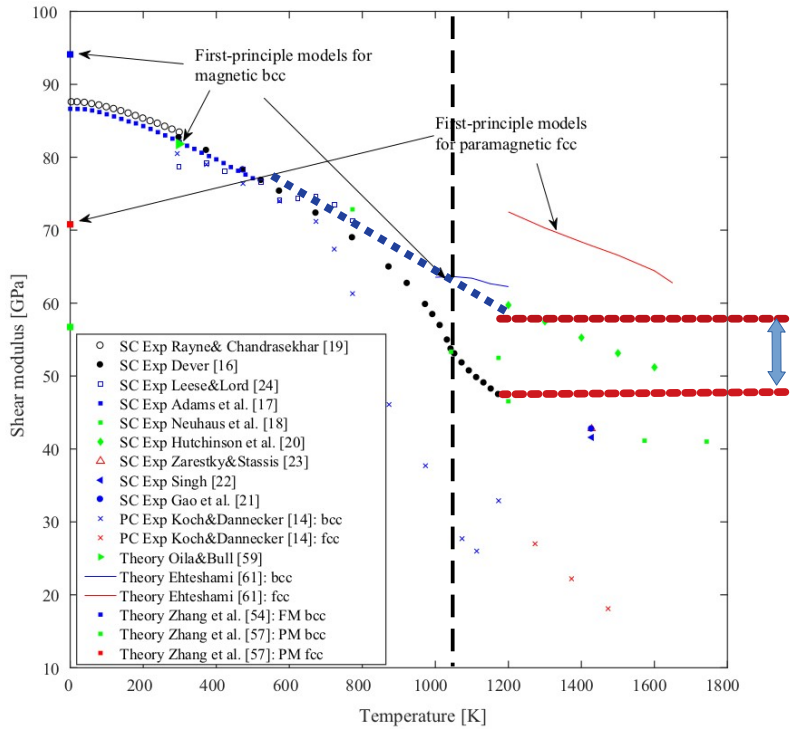

~ 10 GPa difference (~20%)

Global objective:

- Developing a methodology enabling to accurately account for magnetic effects when simulating thermo-mechanical properties of (magnetic) materials.

Relevant for iron, but also for:

- Single-element magnetic metals, steels, HEAs, magnetic oxides, ...

Lindgren, Lars-Erik, and Jessica Gyhlesten Back. "Elastic properties of ferrite and austenite in low alloy steels versus temperature and alloying." Materialia 5 (2019): 100193.

Spin-lattice methodology: a computational model coupling micro-structure and magnetic properties

Molecular Dynamics

- Enables: thermo-mechanical properties, defects, phase-transitions, ...
- Limitations: do not account for magnetization.

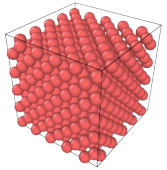

Spin Dynamics

- Enables: magnetization dynamics, spin textures, ...
- Limitations: no structural effects (pressure), fixed lattice.

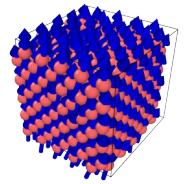

SPIN package, coupled SD - MD

$$\begin{cases} \frac{\partial \boldsymbol{r}_\mathrm{i}}{\partial t} = \boldsymbol{v}_\mathrm{i} \\ \frac{\partial \boldsymbol{v}_\mathrm{i}}{\partial t} = \boldsymbol{F}_\mathrm{i}\left(\boldsymbol{r}_\mathrm{ij}, \boldsymbol{s}_\mathrm{i,j}\right) \\ \frac{\partial \boldsymbol{s}_\mathrm{i}}{\partial t} = \boldsymbol{\omega}_\mathrm{i} \times \boldsymbol{s}_\mathrm{i} \end{cases}$$

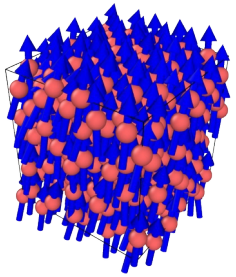

$$\boldsymbol{H}_{sl} = \underbrace{\sum_{i=1}^{N} \frac{|\boldsymbol{p}_i|^2}{2m_i} + \sum_{i,j=1}^{N} V\left(r_{ij}\right)}_{\text{MD Hamiltonian}} \underbrace{- \sum_{i,j,i\neq j}^{N} J\left(r_{ij}\right)\, \boldsymbol{s}_i \cdot \boldsymbol{s}_j - \mu_B \mu_0 \sum_{i=0}^{N} g_i \boldsymbol{s}_i \cdot \boldsymbol{H}_{ext}}_{\text{Spin-lattice coupling}}$$

- All implemented as a LAMMPS package.
- Massively parallel (~ 4X slower than EAM run).
- Nine different magneto-elastic interactions implemented.
- Account for temperature and pressure effects.

J. Tranchida, S. J. Plimpton, P. Thibaudeau, and A.P. Thompson. "Massively parallel symplectic algorithm for coupled magnetic spin dynamics and molecular dynamics." J. of Comp. Phys. 372 (2018): 406-425.

A framework for generating magneto-elastic potentials for iron, leveraging SNAP potentials

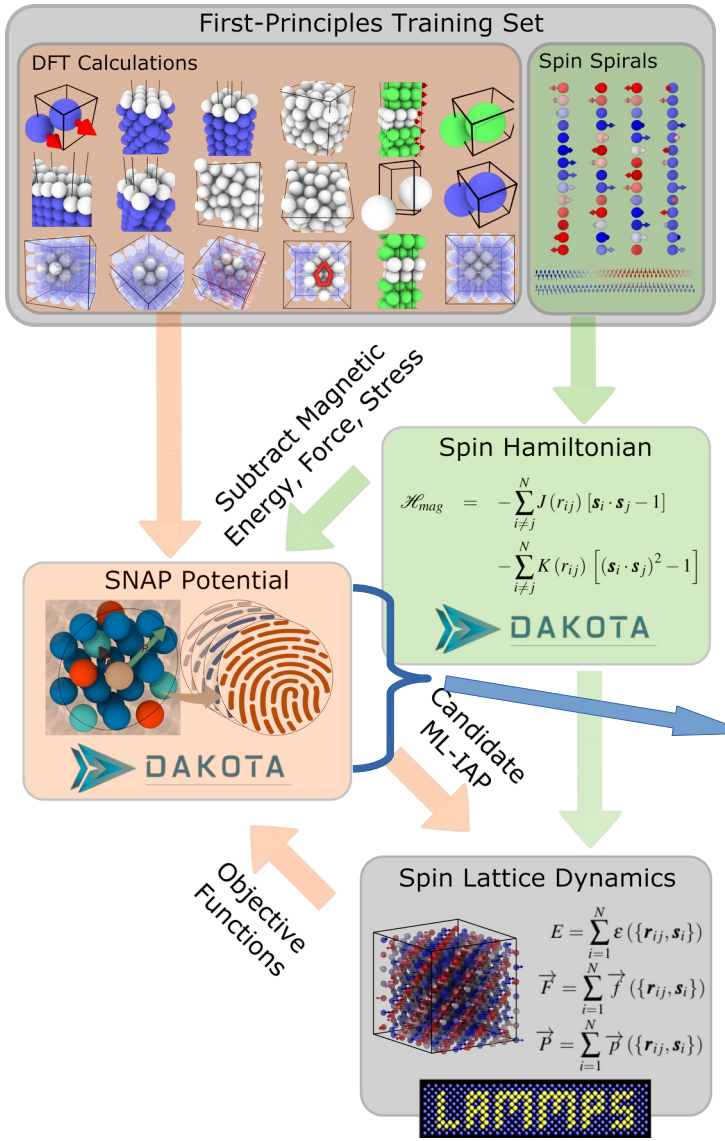

- We leverage the flexibility of the data-driven SNAP methodology to develop accurate magneto-elastic interatomic potentials.
- The DFT training set (DB) consists of spin-spiral calculations and spin-resolved DFT configurations.
- The magneto-elastic potential (Heisenberg type with lattice dependence) is trained first on the spin-spiral results.
- The energies, forces and stress contributions of the magneto-elastic potential are subtracted from the DB. The SNAP potential is trained on this “non-magnetic” DB.
- The two contributions are recombined to generate a 5-N dimensional PES.

[1] Nikolov, Svetoslav, et al. "Data-driven magneto-elastic predictions with classical spin-lattice dynamics." arXiv preprint arXiv:2101.07332 (2021).

First results for alpha-iron

Generating a DB for machine-learning interatomic potential training

- A first iron model is trained on DFT data and some experimental measurements. It corresponds to the following Hamiltonian:

$$\mathcal{H}_{sl} = \sum_{i}^{N} \frac{|\boldsymbol{p}_i|^2}{2m_i} + \sum_{i,j}^{N} V^{SNAP}(\boldsymbol{r}_{ij}) - \sum_{i \neq j}^{N} J\left(r_{ij}\right)\left[\boldsymbol{s}_i \cdot \boldsymbol{s}_j - 1\right] - \sum_{i \neq j}^{N} K\left(r_{ij}\right)\left[\left(\boldsymbol{s}_i \cdot \boldsymbol{s}_j\right)^2 - 1\right],$$

- Zero-temperature measurements of our potential compared to DFT and / or experimental measurements.

- For the rest of this work, 16k atoms proved sufficient to accurately perform temperature dependent measurements.

	SNAP	Exp/DFT	Units	Error %
c_{11}	243.25	239.55	GPa	1.54%
c_{12}	135.65	138.1	GPa	1.77%
c_{44}	118.73	120.75	GPa	1.67%
Bulk modulus	171.52	169.55	GPa	1.16%
$0.5(c_{11}\text{-}c_{12})$	53.8	51.9	GPa	3.66%
Poisson ratio	0.358	0.36	-	1.10%
bcc energy	-8.25	-8.26	eV	0.02%
bcc lat. const.	2.838	2.83	Å	0.30%
hcp energy	-8.10	-8.19	eV	1.10 %
hcp lat. const.	2.506	2.46	Å	1.80%

Nikolov, Svetoslav, et al. "Quantum-accurate magneto-elastic predictions with classical spin-lattice dynamics." arXiv preprint arXiv:2101.07332 (2021).

First results for alpha-iron

Magneto-static accuracy (quantitative agreement with DFT)

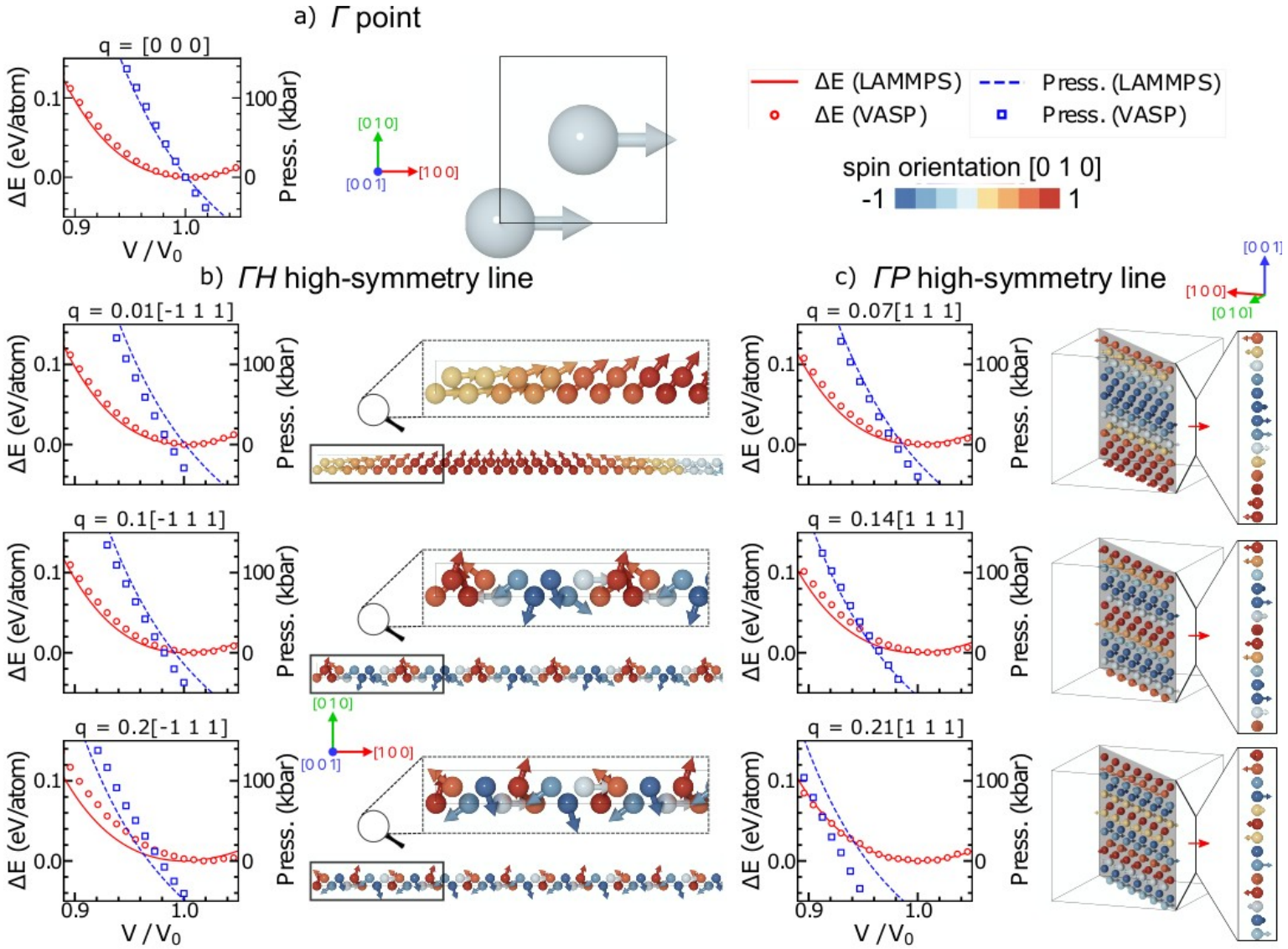

Nikolov, Svetoslav, et al. "Quantum-accurate magneto-elastic predictions with classical spin-lattice dynamics." arXiv preprint arXiv:2101.07332 (2021).

First results for alpha-iron

Magneto-dynamic accuracy (qualitative agreement with experimental measurements)

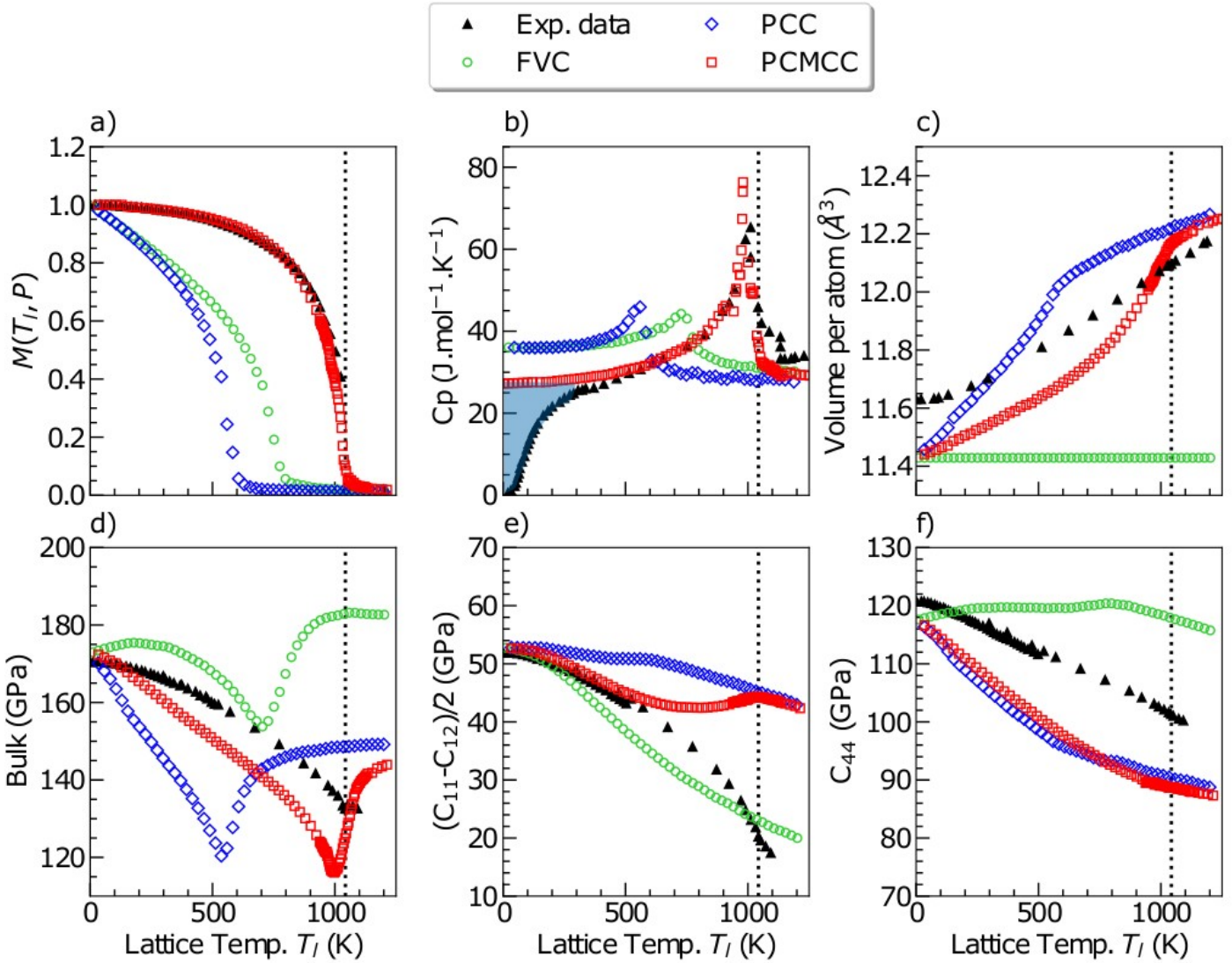

FVC: fixed-volume conditions

PCC: pressure-controlled conditions

PCMCC: pressure-controlled and magnetization-controlled conditions

Nikolov, Svetoslav, et al. "Quantum-accurate magneto-elastic predictions with classical spin-lattice dynamics." arXiv preprint arXiv:2101.07332 (2021).

First results for alpha-iron

Phononic and magnonic thermal conductivity measurements

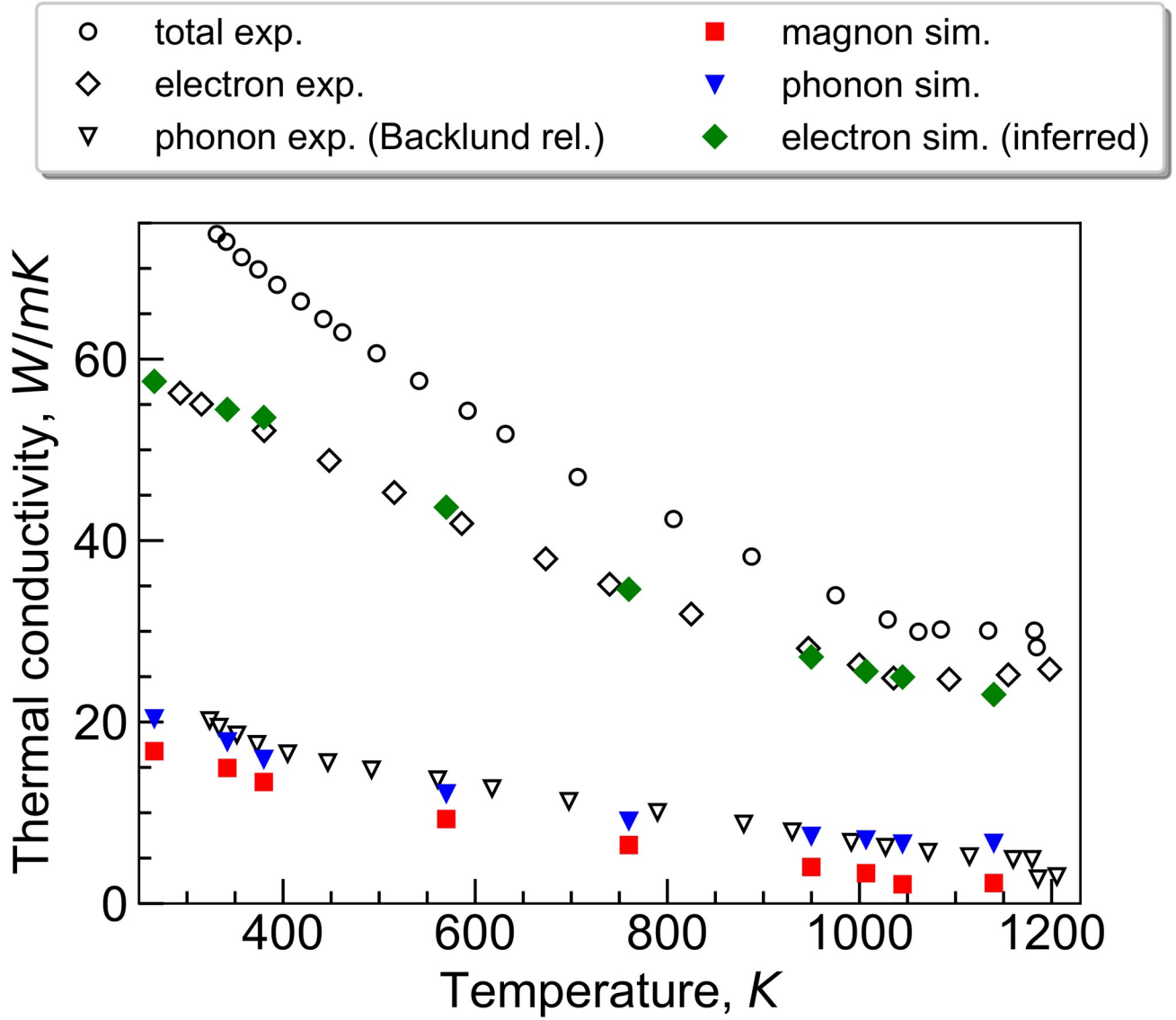

Bäcklund, N. G. "An experimental investigation of the electrical and thermal conductivity of iron and some dilute iron alloys at temperatures above 100 K." Journal of Physics and Chemistry of Solids 20.1-2 (1961): 1-16.

Conclusions

Results:

- A new framework leveraring the SNAP methodology to construct internally consistent, data-driven magneto-elastic interatomic potentials trained on DFT data was developed.
- The framework is applied to iron. We can now generate fully consistent magneto-elastic potentials for alpha-iron, reproducing magnetic and elastic properties.

Perspectives:

- Improving the spin model:
  - Improving the volume-magnetostriction temperature dependence.
  - Accounting for longitudinal spin fluctuations (very important for nickel, or for iron at higher pressure).
  - Means developing new Heinsenberg Hamiltonian (spin-cluster expansion).
- Potential for the alpha -> epsilon and alpha -> gamma transition.
- Applying the approach to different material compositions!

  - Any suggestion welcome, feel free to contact us (jtranch@sandia.gov).

A framework for generating magneto-elastic potentials for iron, leveraging SNAP potentials

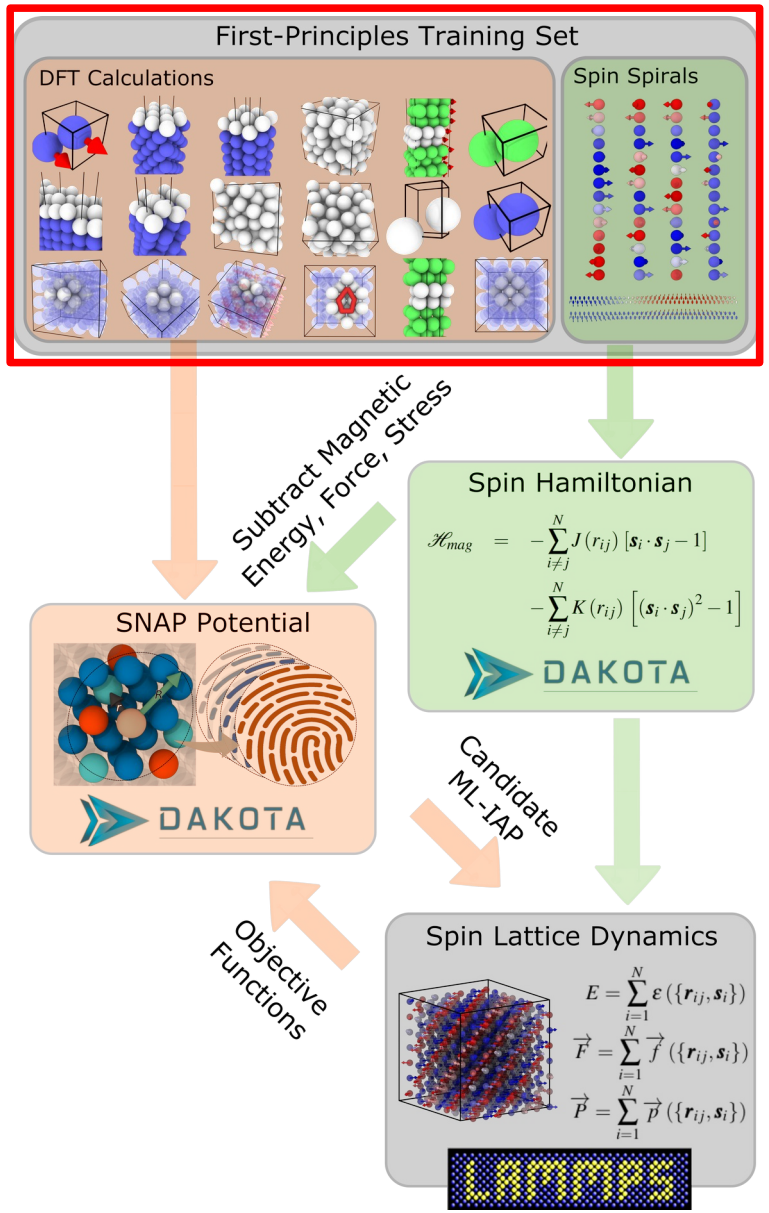

Generating a DB for machine-learning interatomic potential training

- ML-IAP are trained on a DB of atomic configurations:

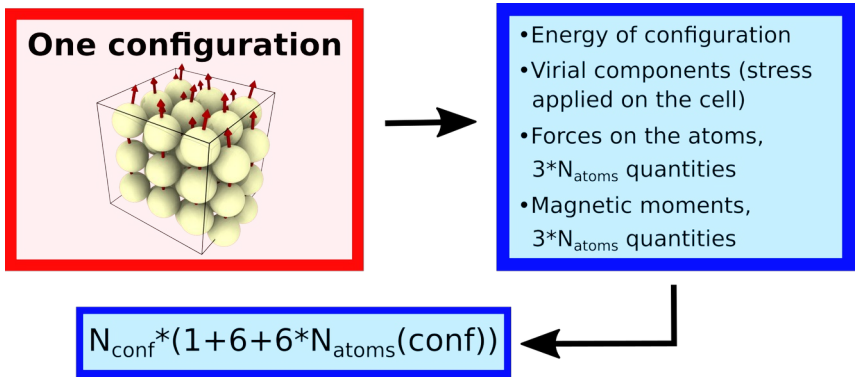

	# of Config.	# of Forces	Target property
Eq. of State	403	65286	Volumetric Deform
DFT-MD, 300K	40	15360	Bulk phonons
Liquid w/ Spins	10	3000	Magnetic Disorder
Liquid w/o Spins	52	15300	Structural Disorder
Point Defects	10	3096	Defect Energetics
BCC, HCP Deform	1477	8148	Elasticity
Martensitic Transform	168	1008	$\alpha \rightarrow \epsilon$

- Each configuration is the result of a self-consistent Density Functional Theory (DFT) calculation (performed with VASP).
- Chosen DFT setup:
  - PBE pseudo-potential
  - Non-collinear, no spin-orbit coupling
  - Smearing corresponding to 300K.

A framework for generating magneto-elastic potentials for iron, leveraging SNAP potentials

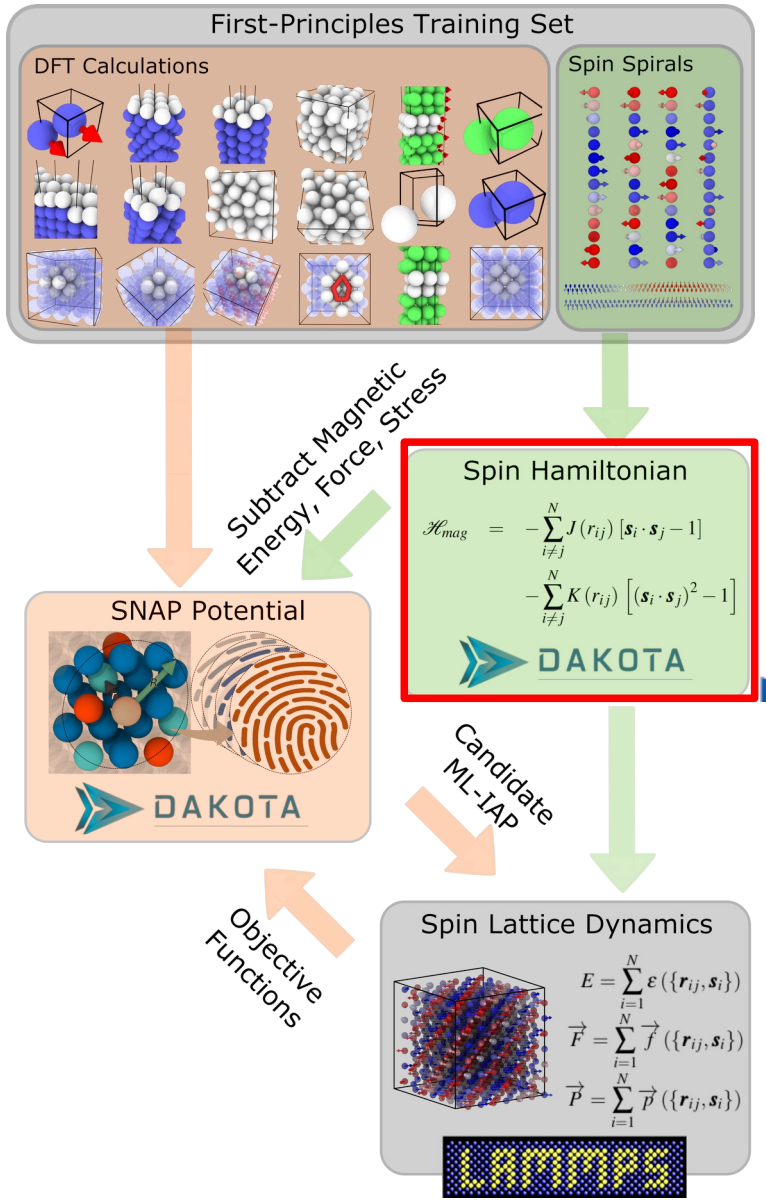

Fitting magnetic interactions on ab-initio results

- We chose an extended Heisenberg Hamiltonian (adding a biquadratic contribution):

$$\mathcal{H}_{mag} = -\sum_{i \neq j}^{N} J\left(r_{ij}\right)\left[\boldsymbol{s}_i \cdot \boldsymbol{s}_j - 1\right] - \sum_{i \neq j}^{N} K\left(r_{ij}\right)\left[\left(\boldsymbol{s}_i \cdot \boldsymbol{s}_j\right)^2 - 1\right],$$

- From this magnetic interaction, per-atom energy and mechanical forces can be computed:

$$E_i = -\sum_{j}^{Neigh} J_{ij}(r_{ij})\left[\boldsymbol{s}_i \cdot \boldsymbol{s}_j - 1\right]$$

$$\boldsymbol{F}_i = \sum_{j}^{Neigh} \frac{d\, J_{ij}(r_{ij})}{d\, r_{ij}}\left[\boldsymbol{s}_i \cdot \boldsymbol{s}_j - 1\right] \boldsymbol{e}_{ij}$$

- Spin-spirals can be generated according to the following expression:

$$\boldsymbol{s}_j = \sin(\theta)\cos(\boldsymbol{q}\cdot\boldsymbol{R}_{0j})\boldsymbol{x} + \sin(\theta)\sin(\boldsymbol{q}\cdot\boldsymbol{R}_{0j})\boldsymbol{y} + \cos(\theta)\boldsymbol{z},$$

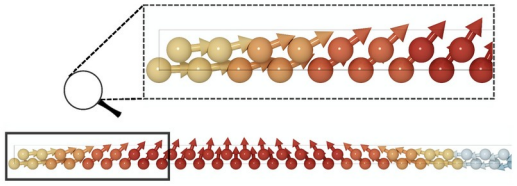

- We use Dakota optimization algorithms to optimize the coefficients of our spin Hamiltonian, so that our LAMMPS spirals (supercells) match the DFT results.

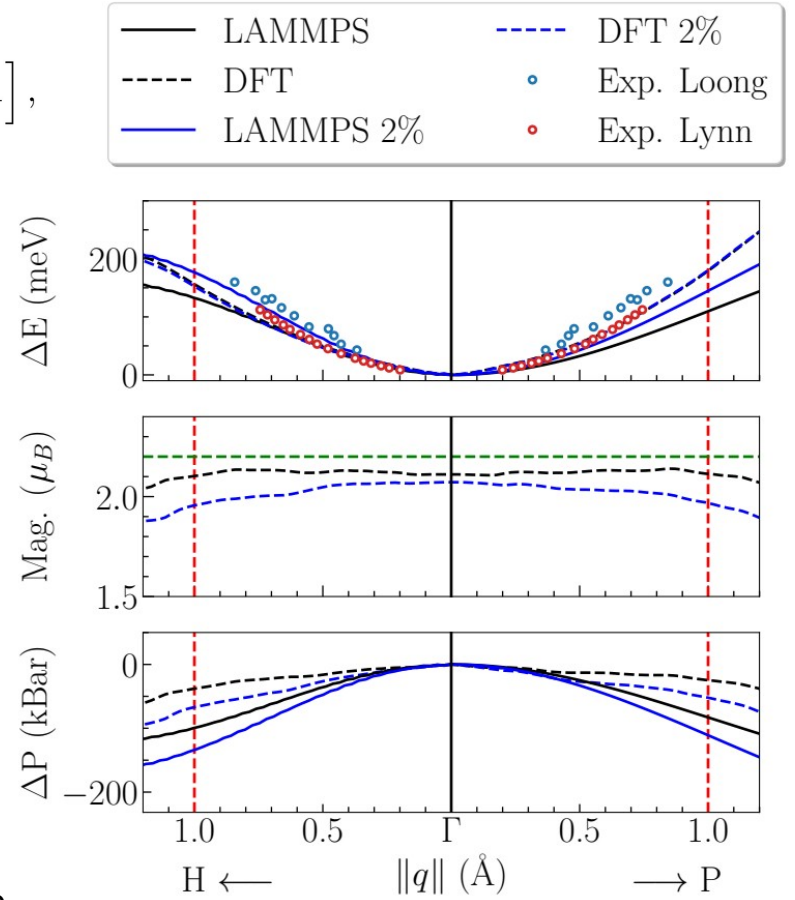

A framework for generating magneto-elastic potentials for iron, leveraging SNAP potentials

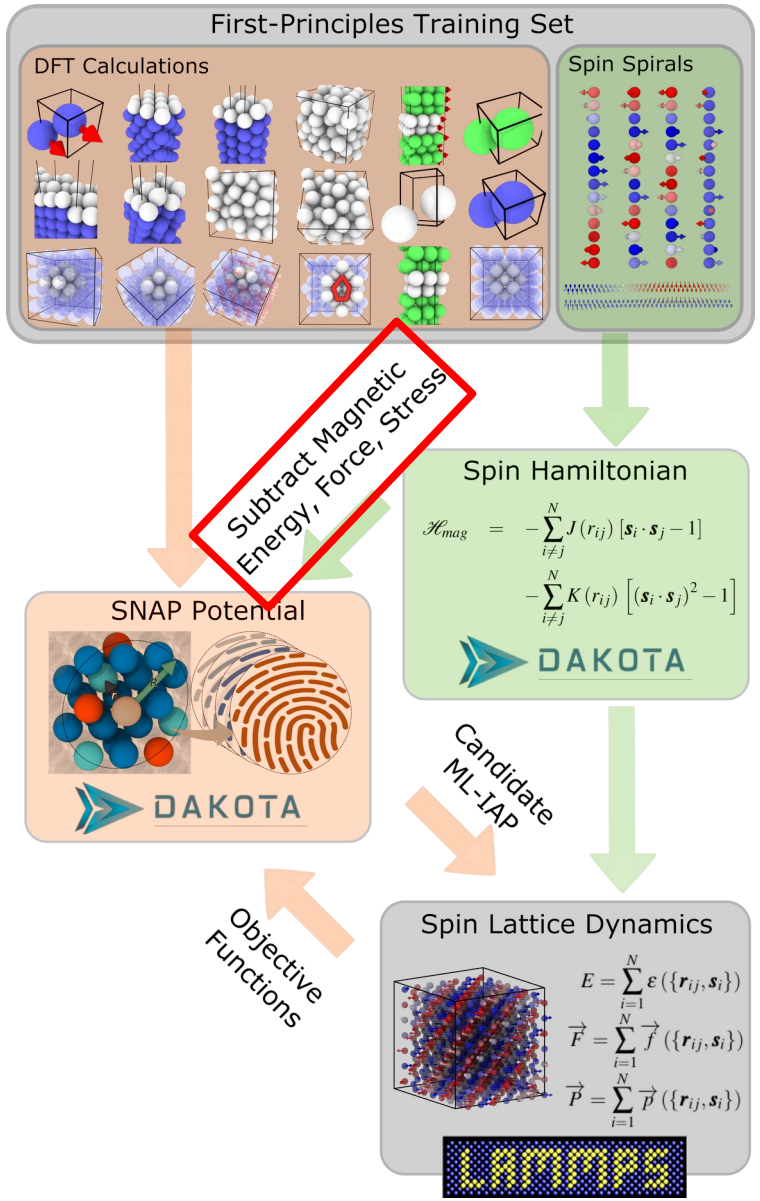

Subtracting the magnetic Hamiltonian from the DB

- The magnetic Hamiltonian is used as a reference potential.
- From each configuration, we subtract the energy, the mechanical forces and virial components generated by the parametrized spin Hamiltonian:

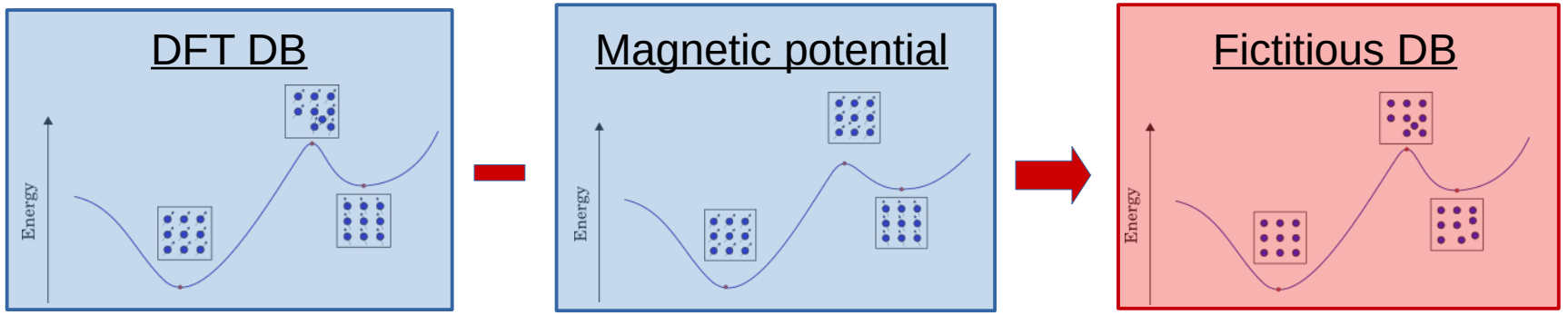

- Generates a fictitious DB, on which we will train a ML-interatomic potential.

$$E_i^{Fic} = E_i^{DFT} - E_i^{Mag}$$

$$\boldsymbol{F}_i^{Fic} = \boldsymbol{F}_i^{DFT} - \boldsymbol{F}_i^{Mag}$$

A framework for generating magneto-elastic potentials for iron, leveraging SNAP potentials

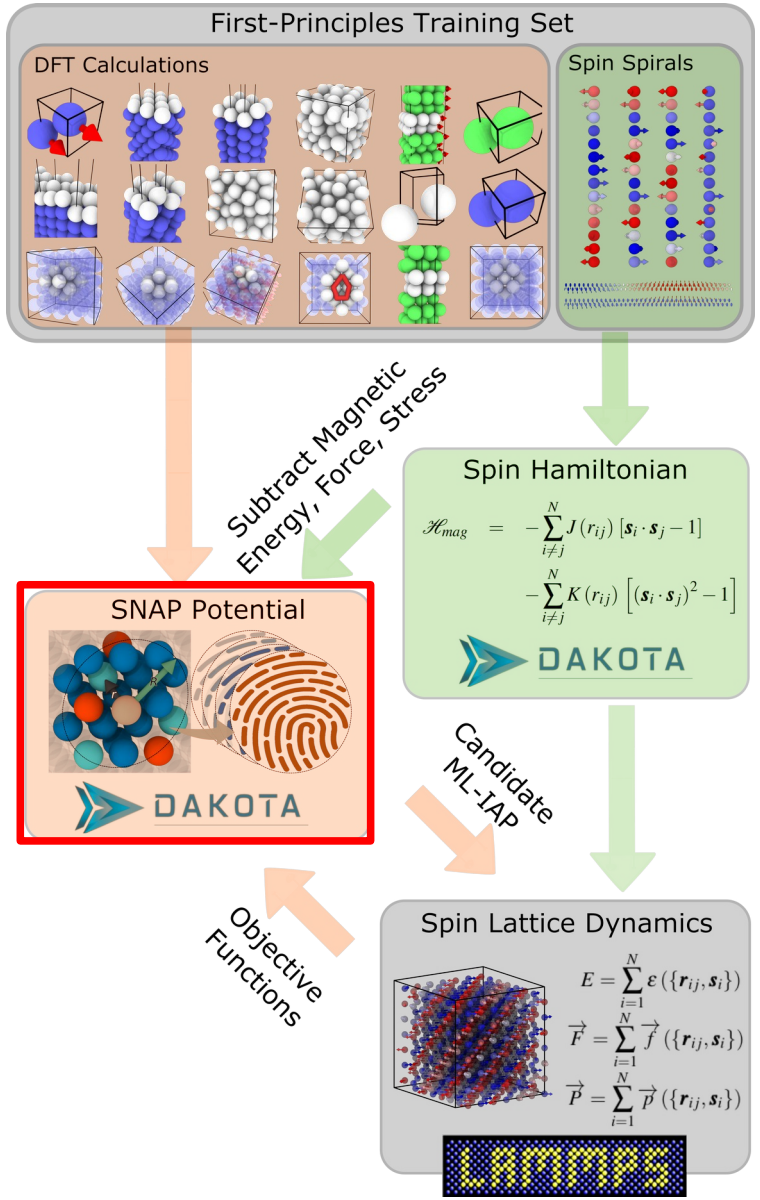

Training a machine-learning interatomic potential on the fictitious PES

- Using the SNAP approach (developed at Sandia, implemented in LAMMPS).
- Energy and forces are expressed in terms of bispectrum components:

$$\begin{cases} E^i_{SNAP} = \beta_0 + \boldsymbol{\beta} \cdot \boldsymbol{B}^i \\ \boldsymbol{F}^j_{SNAP} = -\boldsymbol{\beta} \cdot \sum_{i=1}^{N} \dfrac{\partial \boldsymbol{B}_i}{\partial \boldsymbol{r}_j} \end{cases}$$

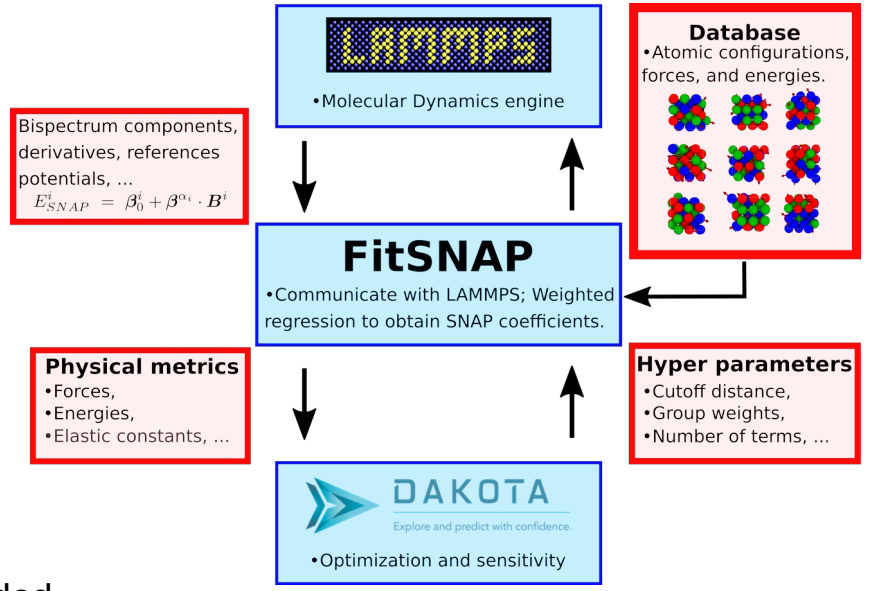

- Twelve additional objective functions were added to the training procedure.

Thompson, Aidan P., et al. "Spectral neighbor analysis method for automated generation of quantum-accurate interatomic potentials." Journal of Computational Physics 285 (2015): 316-330.

A framework for generating magneto-elastic potentials for iron, leveraging SNAP potentials

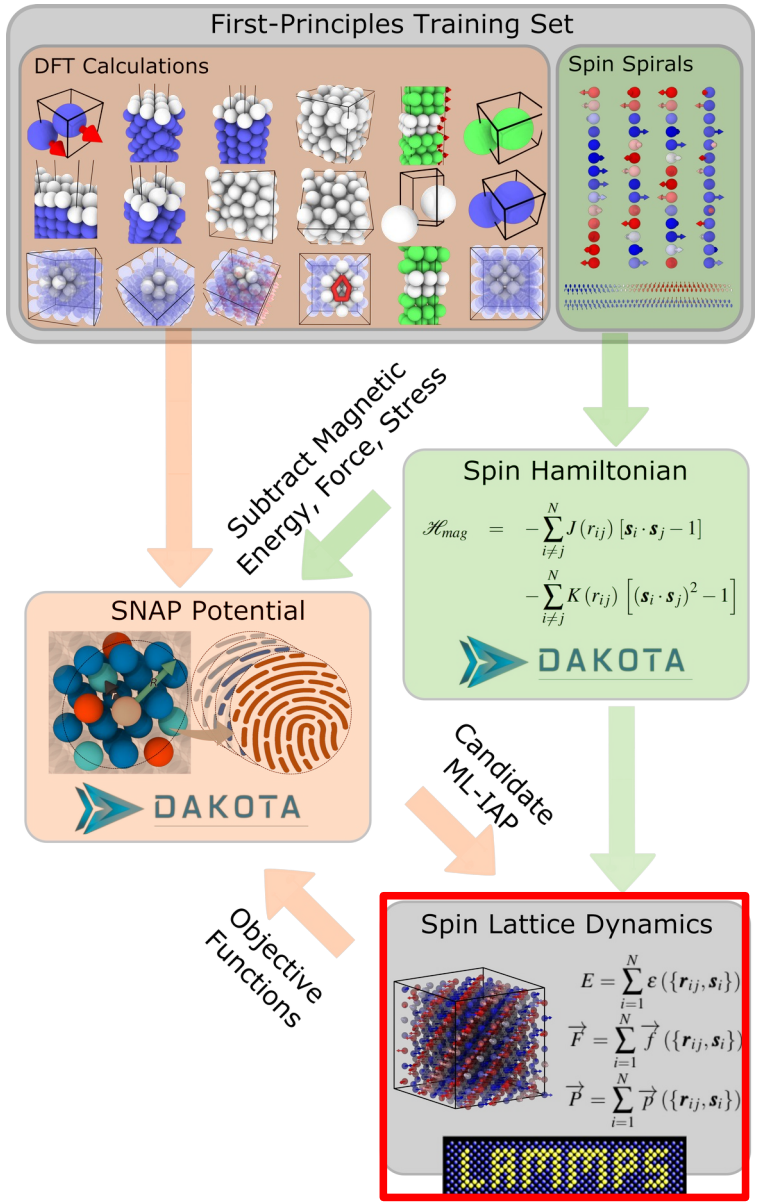

Running SD-MD simulations

- Recombining the contributions of the SNAP and Spin potentials:

$$\mathcal{H}_{sl} = \sum_{i}^{N} \frac{|\boldsymbol{p}_i|^2}{2m_i} + \sum_{i,j}^{N} V^{SNAP}(\boldsymbol{r}_{ij}) - \sum_{i\neq j}^{N} J(r_{ij})\,[\boldsymbol{s}_i\cdot\boldsymbol{s}_j - 1] - \sum_{i\neq j}^{N} K(r_{ij})\left[(\boldsymbol{s}_i\cdot\boldsymbol{s}_j)^2 - 1\right],$$

- Perform spin-lattice simulations with LAMMPS.

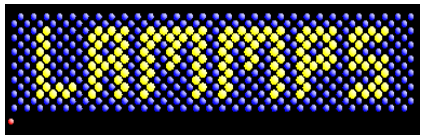

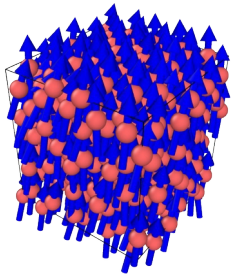

	SNAP	Exp/DFT	Units	Error %
c_{11}	243.25	239.55	GPa	1.54%
c_{12}	135.65	138.1	GPa	1.77%
c_{44}	118.73	120.75	GPa	1.67%
Bulk modulus	171.52	169.55	GPa	1.16%
$0.5(c_{11}-c_{12})$	53.8	51.9	GPa	3.66%
Poisson ratio	0.358	0.36		1.10%
bcc energy	-8.25	-8.26	eV	0.02%
bcc lat. const.	2.838	2.83	Å	0.30%

Nikolov, Svetoslav, et al. "Quantum-accurate magneto-elastic predictions with classical spin-lattice dynamics." arXiv preprint arXiv:2101.07332 (2021).